Concentrations and stable carbon isotope compositions of oxalic acid and related SOA in Beijing before, during and after the 2014 APEC

Jiayuan Wang[1,3], Gehui Wang[1,2,3,4,*], Jian Gao[5,6,*], Han Wang[5,6], Yanqin Ren[1,3], Jianjun Li[1], Bianhong Zhou[1], Can Wu[1,3], Lu Zhang[1,3], Shulan Wang[5,6], Fahe Chai[5,6]

[1]State Key Laboratory of Loess and Quaternary Geology, Key Lab of Aerosol Chemistry and Physics, Institute of Earth Environment, Chinese Academy of Sciences, Xi'an 710061, China
[2]School of Human Settlements and Civil Engineering, Xi'an Jiaotong University, Xi'an 710079, China
[3]University of Chinese Academy of Sciences, Beijing 100049, China
[4]Center for Excellence in Regional Atmospheric Environment, Institute of Urban Environment, Chinese Academy of Sciences, Xiamen 361021, China
[5]State Key Laboratory of Environmental Criteria and Risk Assessment, Chinese Research Academy of Environmental Sciences, Beijing 100084, China
[6]Collaborative Innovation Center of Atmospheric Environment and Equipment Technology, Nanjing 210000, China

Correspondence to: Gehui Wang (wanggh@ieecas.cn) and Jian Gao (gaojian@craes.org.cn)

Abstract: To ensure the good air quality for the 2014 APEC, stringent emission controls were implemented in Beijing and its surrounding regions, leading to a significant reduction in $PM_{2.5}$ loadings. To investigate the impacts of the emission controls on aerosol composition and formation, high-volume $PM_{2.5}$ samples were collected in Beijing from 8th October to 24th November, 2014 and determined for secondary inorganic ions (SIA, i.e., SO_4^{2-}, NO_3^- and NH_4^+), dicarboxylic acids, keto-carboxylic acid and α-dicarbonyls, as well as stable carbon isotope composition of oxalic acid (C_2). Our results showed that SIA, C_2 and related SOA in $PM_{2.5}$ before-APEC were 2−4 times higher than those during-APEC, which can be ascribed to the warm, humid and stagnant conditions before-APEC that are favorable for secondary aerosol production.

C_2 in the polluted air masses, which mostly occurred before-APEC, are abundant and enriched in ^{13}C. On the contrary, C_2 in the clean air masses, which is mostly occurred during-APEC, is much less abundant but still enriched in ^{13}C. In the mixed type of clean and polluted air masses, which mostly occurred after-APEC, C_2 is lower than that before-APEC but higher than that during-APEC and enriched in lighter ^{12}C. A comparison on chemical composition of fine particles and $\delta^{13}C$ values of C_2 in two events that are characterized by high loadings of $PM_{2.5}$ further showed that after-APEC SIA and TDOC are much less abundant and fine aerosols are enriched with primary organics and relatively fresh, compared with those before-APEC.

Key words: Secondary organic aerosols; Emission controls; Sources and formation mechanisms; Aqueous-phase oxidation; Aerosol acidity and water content.

1. Introduction

Atmospheric aerosols profoundly impact the global climate directly by scattering and absorbing solar radiation and indirectly by affecting cloud formation and distribution via acting as cloud condensation nuclei (CCN) and ice nuclei (IN). Moreover, atmospheric aerosols exert negative effects on human health because of their toxicity. Due to fast urbanization and industrialization, high level of atmospheric fine particle ($PM_{2.5}$) pollution has been a persistent problem in many cities of China since the nineties of last century (van Donkelaar et al., 2010). As the capital of China and one of the largest megacities in the world, Beijing has suffered from frequent severe haze pollution especially in winter, affecting more than 21 million people by the end of 2014 (Beijing Municipal Bureau of Statistics, 2015) and causing billions of economic loses (Mu and Zhang, 2013). To improve the air quality Beijing government has put many efforts to reduce the pollutant emissions (i.e., SO_2, NOx, dust, and volatile organic compounds (VOCs)) from a variety of sources.

The 2014 Asia-Pacific Economic Cooperation (APEC) summit was hosted in Beijing from the 5^{th} to 11^{th} November. To ensure good air quality for the summit, a joint strict emission control program was conducted from 3^{rd} November 2014 in Beijing and its neighboring provinces including Inner Mongolia, Shanxi, Hebei and Shandong provinces. During this period thousands of factories and power plants with high emissions were shut down and/or halted, all the construction activities were stopped and the numbers of on-road vehicles were reduced. These strict emission controls resulted in the air quality of Beijing during the APEC period being significantly improved, leading to a decrease in $PM_{2.5}$ concentration by 59.2% and an increase in visibility by 70.2% in Beijing during the summit compared with those before the APEC (Tang et

al., 2015) and a term of "APEC-Blue" being created to refer to the good air quality. Such strong artificial intervening not only reduced $PM_{2.5}$ and its precursors' loadings in Beijing and its surrounding areas but also affected the composition and formation mechanisms of the fine particles (Sun et al., 2016).

A number of field measurements have showed that particle compositions in Beijing during wintertime haze periods are dominated by secondary aerosols (Guo et a., 2014; Huang et al, 2014; Xu et al., 2015). Rapid accumulation of particle mass in Beijing during haze formation process is often accompanied by continuous particle size growth (Guo et al, 2014; Zhang et al., 2015), which is in part due to the coating of secondary organic aerosols (SOA) on pre-existing particles (Li et al., 2010). Several studies have found that SOA production during the 2014 Beijing APEC periods significantly reduced and ascribed this reduction to the efficient regional emission control (Sun et al., 2016; Xu et al, 2015). However, up to now information of the SOA decrease on a molecular level has not been reported. Dicarboxylic acids are the major class of SOA species in the atmosphere and ubiquitously found from the ground surface to the free troposphere (Fu et al., 2008; Myriokefalitakis et al., 2011; Sorooshian et al., 2007; Sullivan et al., 2007). In the current work we measured molecular distributions of dicarboxylic acids, keto-carboxylic acids and α-dicarbonyls and stable carbon isotope composition of oxalic acid in $PM_{2.5}$ aerosols collected in Beijing before, during and after the APEC event in order to explore the impact of the APEC emission control on SOA in Beijing. We first investigated the changes in concentration and composition of dicarboxylic acids and related compounds during the three periods, then recognized the difference in stable carbon isotope composition of oxalic acid in different air masses in Beijing during the APEC campaign. Finally we compared the different

chemical and compositions of $PM_{2.5}$ during two heaviest pollution episodes.

2. Experimental section

2.1 Sample collection

$PM_{2.5}$ samples were collected by using a high-volume sampler (Brand, USA) from 8th October to 24th November 2014 on the rooftop of a three-storey building located on the campus of China Research Academy of Environmental Sciences, which is situated in the north part of Beijing and close to the 5th-ring road. All the $PM_{2.5}$ samples were collected onto pre-baked (450 ^{o}C for 8 h) quartz fiber filters (Whatman 41, USA). The duration of each sample collection is 23 hr from 08:00 am of the previous day to 07:00 am of the next day. Field blanks were also collected before and after the campaign by mounting a pre-baked filter onto the sampler for 15 min without pumping air. After collection, all the filter samplers were individually sealed in aluminum foil bags and stored in a freezer (-18 ^{o}C) prior to analysis. Daily values of SO_2, NOx and meteorological parameters were cited from the website of Beijing Environmental Protection Agency.

2.2 Sample analysis

2.2.1 Elemental carbon (EC), organic carbon (OC), water-soluble organic (WSOC), inorganic ions, aerosol liquid water content (ALWC) and aerosol acidity.

Detailed methods for the analysis of EC, OC, WSOC and inorganic ions in aerosols were reported elsewhere (Li et al., 2011; Wang et al 2010). Briefly, EC and OC in the $PM_{2.5}$ samples were determined by using DRI Model 2001 Carbon analyzer following the Interagency Monitoring of Protected Visual Environments (IMPROVE) thermal/optical reflectance (TOR) protocol (Chow et al., 2007). WSOC and inorganic ions in the samples were extracted with

Milli-Q pure water and measured by using Shimadzu TOC-L CPH analyzer and Dionex-600 ion chromatography, respectively (Li et al. 2011; Wang et al 2010). In the current work, aerosol liquid water content (ALWC) and acidity (i.e., liquid H^+ concentrations, $[H^+]$) of the samples were calculated by using ISORROPIA-II model, which treated the $Na^+–NH_4^+–K^+–Ca^{2+}–Mg^{2+}–Cl^-–NO_3^-–SO_4^{2-}$ system and was performed in a "metastable" mode (Hennigan et al, 2015; Weber et al., 2016).

2.2.2 Dicarboxylic acids, keto-carboxylic acids and α-dicarbonyls

The method of analyzing $PM_{2.5}$ samples for dicarboxylic acids, ketocarboxylic acids and α-dicarbonyl has been reported elsewhere (Wang et al., 2002, 2012; Meng et al., 2014; Cheng et al., 2015). Briefly, one eighth of the filter was extracted with Milli-Q water, concentrated to near dryness, and reacted with 14% BF_3/butanol at 100 °C for 1 h to convert aldehyde group into dibutoxy acetal and carboxyl group into butyl ester. Target compounds in the derivatized samples were identified by GC/MS and quantified by GC-FID (Agilent GC7890A).

2.3. Stable carbon isotope composition of oxalic acid (C_2)

Stable carbon isotope composition ($\delta^{13}C$) of C_2 was measured using the method developed by Kawamura and Watanabe (2004). Briefly, $\delta^{13}C$ values of the derivatized samples above were determined by gas chromatography-isotope ratio-mass spectrometry (GC-IR-MS) (Thermo Fisher, Delta V Advantage). The $\delta^{13}C$ value of C_2 was then calculated from an isotopic mass balance equation based on the measured $\delta^{13}C$ of the derivatizations and the derivatizing reagent (1-butanol) (Kawamura and Watanabe, 2004). Each sample was measured for three times to ensure the difference of the $\delta^{13}C$ values less than 0.2‰, and the isotope data reported here is the averaged value of the triplicate measurements.

3. Results and discussion

3.1 Variations in meteorological conditions, gaseous pollutants and major components of $PM_{2.5}$ during the Beijing 2014 APEC campaign

Based on the emission control implementation for the APEC, we divided the whole study period into three phases: before-APEC (08/10 to 02/11), during-APEC (03/11 to 12/11) and after-APEC (13/11 to 24/11). Temporal variations in meteorological parameters and concentrations of gaseous pollutants and major components of $PM_{2.5}$ during the three phases are shown in Fig. 1 and summarized in Table 1.

Temperature during the sampling campaign showed a continuous decreasing trend with averages of 13 ± 2.6 °C, 7.0 ± 1.7 °C and 4.3 ± 1.3 °C before-, during- and after-APEC periods, respectively, while relative humidity (RH) did not show a clear trend with mean values of 62 ± 19%, 47 ± 14% and 51 ± 16% during the three periods (Fig.1a and Table 1). SO_2 showed a similar level before- and during-APEC periods (8.8 ± 4.6 μg m^{-3} versus 7.6 ± 3.9 μg m^{-3}) (Table 1), but increased dramatically to 23 ± 8.8 μg m^{-3} after-APEC due to domestic coal burning for house heating (Fig. 1b). NO_2 concentration (45 ± 18 μg m^{-3}) during the APEC reduced by about 30% compared to that in the before- and after-APEC phases (71 ± 27 μg m^{-3} versus 78 ± 29 μg m^{-3}) (Table 1), mainly because of the reduction of the on-road vehicle numbers, as well as the reduced productivities of power plant and industry. O_3 displayed a decreasing trend similar to that of temperature (Fig. 1c). $PM_{2.5}$ pollution episodes in Beijing showed a periodic cycle of 4−5 days, which is caused by the local weather cycles. Secondary inorganic ions (SIA, i.e., SO_4^{2-}, NO_3^- and NH_4^+) are major components of $PM_{2.5}$ and present a temporal variation pattern similar to that of the fine particles (Fig. 1d). In the current work mass ratio of NO_3^-/SO_4^{2-} in $PM_{2.5}$

during the whole study time is 1.8 ± 1.9 (Table 1), which is in agreement with the ratio (1.6−2.4) for PM_1 observed during the same time by using aerosol mass spectrometry (AMS) (Sun et al., 2016). OC and EC of $PM_{2.5}$ linearly correlated each other (R^2=0.91) and varied periodically in a cycle similar to SIA (Fig. 1e). OC/EC ratio during the whole sampling period is 3.3 ± 0.6 (range: 2.2−4.7) with no significant differences among the three APEC phases (Table 1).

Figure 2 shows the differences in chemical composition of $PM_{2.5}$ before-, during- and after-APEC periods. $PM_{2.5}$ is 98 ± 46 μg m^{-3} during-APEC, about 50% lower than that before- and after-APEC (178 ± 122 μg m^{-3} versus 161 ± 100 μg m^{-3}), respectively. Organic matter (OM) is the most abundant component of the fine particles. Relative abundance of OM (OM, 1.6 times of OC) (Xing et al., 2013) to $PM_{2.5}$ continuously increaseed from 24% before-APEC to 30% and 39% during- and after-APEC, respectively, although the mass concentration (19 ± 7.6 μg m^{-3}) of OC during-APEC is the lowest compared to those before- and after-APEC (26 ± 16 μg m^{-3} versus 39 ± 23 μg m^{-3}). Sulfate, nitrate and ammonium before-APEC are 15 ± 13, 28 ± 26 and 9.0 ± 8.0 μg m^{-3} (Table 1) and account for 8%, 16% and 5% of $PM_{2.5}$, respectively (Fig. 2). Their concentrations decrease to 5.3 ± 2.8, 10 ± 8.1 and 3.1 ± 2.6 μg m^{-3} (Table 1) with the relative contributions to $PM_{2.5}$ down to 5%, 10% and 3% during-APEC, respectively. While after-APEC their concentrations increased to 11 ± 10, 15 ± 13 and 6.9 ± 6.4 μg m^{-3} and accounted for 7%, 9% and 4% of $PM_{2.5}$. Such significant decreases in concentrations of OM and SIA during-APEC demonstrate the efficiency of the emission controls. OC/EC ratio is almost constant during the whole period, but WSOC/OC ratio decreased by 20% from 0.42 ± 0.13 before-APEC, 0.38 ± 0.16 during-APEC to 0.35 ± 0.17 after-APEC (Table 1). Since WSOC in fine aerosols consist mainly of secondary organic aerosols (SOA) (Laskin et al., 2015), the decreasing ratio of

196 WSOC/OC probably indicates a reduced SOA production during the campaign.

197 **3.2 Oxalic acid and related SOA during the Beijing 2014 APEC campaign**

198 A homogeneous series of dicarboxylic acids (C_2−C_{11}), keto-carboxylic acid and
199 α-dicarbonyls in the $PM_{2.5}$ samples were detected. As show in Table 2, total dicarboxylic acids
200 during the whole study period is 593 ± 739 ng m^{-3}, which is lower than that observed during
201 Campaign of Air Quality Research in Beijing 2006 (CAREBeijing) (average 760 ng m^{-3}) and
202 2007 (average 1010 ng m^{-3}) (Ho et al, 2010, 2015) and the averaged wintertime concentration
203 reported by a previous research for 14 Chinese cities (904 ng m^{-3}) (Ho et al, 2007). Total
204 keto-carboxylic acid is 66 ± 81 ng m^{-3}, while total dicarbonyls is 126 ± 115 ng m^{-3} (Table 2).
205 These values are higher than those during CAREBeijing 2006 and 2007 (Ho et al, 2010, 2015),
206 but close to the value observed for the 14 Chinese megacities (Ho et al, 2007). Being similar to
207 those previous observations, oxalic acid (C_2) is the most abundant diacid in the 2014 APEC
208 samples with an average of 334 ± 461 ng m^{-3} (range: 10−2127 ng m^{-3}, Table 2) during the whole
209 campaign, followed by methylglyoxal (mGly), succinin acid (C_4), terephthalic acid (tPh), and
210 glyoxal (Gly). These five species account for 43%, 10%, 9%, 6% and 6% of total detected
211 organic compounds (TDOC), respectively (Fig. 3).

212 As see in Fig. 4, TDOC in $PM_{2.5}$ are 1099 ± 1104, 325 ± 220 and 487 ± 387 ng m^{-3} before-,
213 during- and after-APEC, respectively. In comparison with those before-APEC, TDOC
214 during-APEC decreased by 71%. Oxalic acid (C_2) is the leading species among the detected
215 organic compounds and accounted for 46%, 31% and 34% of TDOC during the three phases,
216 respectively (Fig. 4). C_2 is an end product of precursors that are photochemically oxidized in
217 aerosol aqueous phase via either oxidation of small compounds containing two carbon atoms or

decomposition of larger compounds containing three or more carbon atoms. Thus mass ratio of C_2 to TDOC is indicative of aerosol aging (Wang et al., 2012; Ho et al., 2015). As shown in Fig. 4, the highest proportion of C_2 before- APEC suggests that organic aerosols during this period are more oxidized, compared to those during- and after-APEC. Glyoxal (Gly) and methylglyoxal (mGly) are the precursors of C_2. Mass ratios of both compounds to TDOC are lowest before-APEC (Fig. 4), further indicating an enhanced SOA production during this period.

3.3 Formation mechanism of oxalic acid

3.3.1 Correlation of oxalic acid with temperature, relative humidity (RH), aerosol liquid water content (ALWC) and acidity and sulfate

A few studies have pointed out that aerosol aqueous phase oxidation is a major formation pathway for oxalic acid (Yu et al., 2005; Pinxteren, et al., 2014; Bikkina et al., 2015; Tilgner et al, 2010). To explore the formation mechanism of oxalic acid, we calculated ALWC and acidity (i.e., proton concentration, $[H^+]$) of $PM_{2.5}$ aerosols by using ISOROPPIA-II model (Weber et al., 2016). As shown in Fig. 5, during the entire period C_2 showed a strong linear correlation with sulfate (R^2=0.70 Fig. 5a), which is consistent with those observed in Xi'an (Wang et al., 2012) and other Chinese cities (Yu et al, 2005). Previous studies on particle morphology showed that sulfate particles internally mixes with SOA in Beijing especially in humid haze days (Li et al., 2010, 2011), which probably indicates that they are formed via similar aqueous phase pathways. In addition, a robust correlation was also found for C_2 with RH (R^2=0.64, Fig. 5b) and aerosol liquid water content (ALWC) (R^2=0.61, Fig. 5c), indicating that humid conditions are favorable for the aqueous phase formation of C_2, which is most likely due to an enhanced gas-to-aerosol

aqueous phase partitioning of the precursors (e.g., Gly and mGly) (Fu et al., 2008; Wang et al., 2015).

NH_4^+, NO_3^- and SO_4^{2-} are the dominant cation and anions of fine particles in Beijing, respectively (Guo et al., 2014; Zhang et al., 2015) and the molar ratio of $[NH_4^+]$ to $[NO_3^- + SO_4^{2-}]$ in this study is 1.1. Thus it is plausible that SO_4^{2-} during the APEC campaign largely existed as ammonium bisulfate, resulting in a strong linear correlation between $[H^+]$ and SO_4^{2-} with a molar slope of 1.03 (Fig. 5d) (Zhang et al., 2007). In addition, $[H^+]$ shows a significant positive correlation with C_2 ($R^2 = 0.84$) (Fig. 5e), possibly due to the fact that acidic conditions are favorable for the formation of C_2 precursors. For example, Surratt et al (2007; 2010) found that aerosol acidity can promote the formation of biogenic SOA (BSOA) derived from isoprene oxidation such as 2-methylglyceric acid, Gly and mGly. These BSOA precursors can be further oxidized into C_2 (Meng et al., 2014; Wang et al., 2009).

There is a significant positive correlation ($R^2 = 0.58$, $p<0.001$) between the mass ratios of C_2/TDOC and ambient temperatures (Fig. 5f), which is similar to the results found by previous researchers (Ho et al., 2007; Strader et al., 1999), indicating that organic aerosols are more aged under a higher temperature condition (Erven et al, 2011; Carlton et al., 2009). Thus, compared with those before-APEC the lower C_2/TDOC ratios (31% and 34%, respectively) (Fig. 4) during- and after-APEC can be ascribed in part to the relatively lower temperature conditions that are not favorable for oxidation of the precursors to produce oxalic acid (13 ± 2.6 °C, 7.0 ± 1.7 °C and 4.3 ± 1.3 °C before-, during- and after-APEC periods, respectively) (Table1).

3.3.2 Temporal variation in stable carbon isotopic composition of oxalic acid

To further discuss the formation mechanism of C_2, we investigated the temporal variations

of concentration and stable carbon isotopic composition of C_2 in the $PM_{2.5}$ samples (Fig. 6). Previous studies have demonstrated that Gly, mGly, glyoxylic acid (ωC_2) and pyruvic acid (Pyr) are the precursors of C_2 (Carlton et al., 2006, 2007; Ervens and Barbara, 2004; Wang et al., 2012). Thus, higher mass ratios of C_2 to its precursors indicate that organic aerosols are more oxidized (Wang et al., 2010). As shown in Table 3, $\delta^{13}C$ of C_2 in this work positively correlated with the mass ratios of $C_2/\omega C_2$, C_2/mGly and TDOC/WSOC, demonstrating an enrichment of ^{13}C during the aerosol oxidation process. Because decomposition (or breakdown) of larger molecular weight precursors in aerosol aqueous phase is the dominant formation pathway for C_2 in aerosol ageing process (Kawamura et al., 2016; Gensch et al., 2014; Kirillova et al., 2013), during which organic compounds release CO_2/CO by reaction with OH radical and other oxidants, resulting in the evolved species enriched with lighter isotope (^{12}C) and the remaining substrate enriched in ^{13}C due to kinetic isotope effects (KIE) (Hoefs, 1997; Rudolph et al., 2002).

72-h backward trajectory analysis showed that air masses moved to Beijing during the whole sampling period can roughly be categorized into three types (Fig. 6a) (all trajectories during the entire study period can be found in the supplementary materials). (1) Polluted type, by which air masses originated from inland and east coastal China and moved slowly into Beijing within 72-h from its south regions, i.e., Henan, Shandong and Jiangsu Provinces. This type of air masses mostly occurred before-APEC with high $PM_{2.5}$ concentrations. Air pollution has widely distributed in the three provinces (Wei et al., 2016); thus aerosols transported by this type of air masses are of regional characteristics. (2) Mixed type, by which air masses originated from Mongolia and North China, and moved quickly into Hebei province and then turned back to Beijing. Air in Mongolia and North China was clean but polluted in Hebei province, which is

adjacent to Beijing. This type of air masses is a mixture of clean and polluted air and thus named as mixed type. Since the resident time of the mixed type of air masses within Hebei province is very short, thus aerosols transported by this type of air masses is of local characteristics and relatively fresh. (3) Clean type, by which air masses originated from Siberia and moved rapidly into Beijing directly via a long-range transport. Aerosols from the clean type of air masses are much more aged, while those from the mixed type of air masses are fresh. Since severe air pollution is widespread in the south regions, gas-to-aerosol phase partitioning of precursors and subsequent aerosol-phase oxidation to produce SOA including C_2 continuously proceed during the air mass movement. However, such a partition for producing SOA is not significant when air mass move from Siberia, Mongolia and North China because of the much less abundant VOCs. In stead, aerosols in the clean air masses are continuously oxidized, during which C_2 is produced by photochemical decomposition of larger molecular weight precursors. Therefore, C_2 in $PM_{2.5}$ transported by the mixed type air masses are not only fresh and abundant but also enriched in ^{12}C, whereas C_2 in $PM_{2.5}$ transported by the clean type air masses are aged, less abundant and enriched in ^{13}C due to KIE effects, as illustrated by the pink and light blue columns in Fig. 6b, respectively. C_2 in $PM_{2.5}$ transported by the polluted type of air masses are most abundant compared with that in other two type of air masses, which is not only due to the severe air pollution in the Henan, Shandong and Jiangsu provinces but also due to the enhanced photochemical oxidation under the humid, higher temperature and stagnant conditions that occurred mostly before-APEC, as discussed previously. Therefore, C_2 in the polluted type of air masses is not only abundant but also enriched in ^{13}C (see black columns in Fig. 6b).

3.4 Different chemical characteristics of $PM_{2.5}$ between two severe haze events

From Fig. 1 and Table 4, it can be found that $PM_{2.5}$ showed two equivalent maxima on 9th October and 20th November during the whole study period. However, the chemical compositions of $PM_{2.5}$ during these two pollution events were significantly different. As shown in Fig. 7a, relative abundances of SIA (sum of SO_4^{2-}, NO_3^- and NH_4^+) to $PM_{2.5}$ are 30% during the event I and 23% during the event II, respectively. The relative abundance of OM (21%, Fig. 7a) during the event I is lower than that (37%) during the event II (Fig. 7b). In contrast, the ratios of WSOC/OC and TDOC/OC are higher in the event I than in the event II, which is consistent with lower levels of O_3 after-APEC (Table 1), suggesting a weaker photochemical oxidation capacity during the event II. Organic biomarkers in the $PM_{2.5}$ have been measured for the source apportionment (Wang et al., 2016) and citied here to further identify the difference in chemical composition of $PM_{2.5}$ between the two events. Levoglucosan is a key tracer for biomass burning smoke. Mass ratio of levoglucosan to OC in $PM_{2.5}$ (Lev/OC) is comparable between the two events, suggesting a similar level of contributions of biomass burning emission to $PM_{2.5}$ before- and after-APEC. However, the mass ratios of PAHs and hopanes to OC are lower in event I than those in event II (Fig. 7c), which again demonstrates the enhanced emissions from coal burning for house heating, because these compounds are key tracers of coal burning smokes (Wang et al., 2006). As seen in Fig. 7d, C_2 in the event I was enriched in ^{13}C. Such relatively more abundant SIA, WSOC and TDOC and heavier C_2 in $PM_{2.5}$ clearly demonstrate that $PM_{2.5}$ during the event I were enriched with secondary products while the fine particles during the event II were enriched with primary compounds. After-APEC house heating activities including residential coal burning were activated, which emitted huge amounts of SO_2, NOx, and VOCs as well as primary particles, resulting in both absolute concentrations and relative abundances of CO and

EC 30−40% higher after-APEC than before-APEC (see Table 1). Li et al (2015) reported that VOCs in Beijing was 86 ppbv before-APEC, 48 ppbv during-APEC and 73 ppbv after-APEC. As shown in Table 4, temperature (16.7±0.8 ^{o}C for event I and 4.5±1.7 ^{o}C for event II) and relative humidity (RH) (82±4% for event I and 62±13% for event II) are lower during the event II than during the event I. Moreover, air masses arriving in Beijing during the event II are the mix type, of which the resident time in Hebei province is short. Compared with those in the event I, such colder and drier conditions and short reaction time during the event II are unfavorable for photochemical oxidation, resulting in SOA not only less abundant but also enriched with lighter ^{12}C during the event II, although VOCs levels are comparable before- and after-APEC.

4. Summary and conclusion

Temporal variations in molecular distribution of SIA, dicarboxylic acids, ketoacids and α-dicarbonyl and stable carbon isotopic composition (δ^{13}C) of C_2 in $PM_{2.5}$ collected in Beijing before-, during- and after- the 2014 APEC were investigated. Absolute concentrations and relative abundances of SIA and C_2 in $PM_{2.5}$ are highest before-APEC, followed by those after- and during-APEC, suggesting that the fine aerosols before-APEC are enriched with secondary products, mainly due to an enhanced photochemical oxidation under the warm, humid and stagnant conditions. Concentrations of SIA, oxalic acid and related SOA in $PM_{2.5}$ during-APEC are 2−4 times lower than those before-APEC, which can be ascribed to the effective emission controls and the favorable meteorological conditions that brought clean air from Siberia and Mongolia into Beijing.

Positive correlations of C_2 with RH, sulfate mass, ALWC and aerosol acidity indicate that C_2 formation pathway is involved an acid-catalyzed aerosol aqueous phase oxidation. SIA, C_2

and related SOA in the polluted type of air masses are abundant with C_2 enriched in ^{13}C. On the contrary, those in the clean type of air masses are much less abundant, although C_2 is also enriched in ^{13}C. By comparing the chemical composition of $PM_{2.5}$ and $\delta^{13}C$ values of C_2 in two events that are characterized by the highest loadings of $PM_{2.5}$ before- and after-APEC, we further found that compared with those before- APEC fine aerosols after-APEC are enriched with primary species and C_2 is depleted in heavier ^{13}C, although SO_2, NOx and VOCs are abundant during the heating season, again demonstrating the important role of meteorological conditions in the secondary aerosol formation process, which are warmer, humid and stagnant before-APEC and result in secondary species much more abundant than those during- and after-APEC.

Acknowledgements

This work was financially supported by the Strategic Priority Research Program of the Chinese Academy of Sciences (Grants No. XDB05020401), the China National Natural Science Founds for Distinguished Young Scholars (Grants No. 41325014), and the program from National Nature Science Foundation of China (No. 41405122, 91544226 and 41375132).

References

Bikkina, S., Kawamura, K., and Miyazaki, Y.: Latitudinal distributions of atmospheric dicarboxylic acids, oxocarboxylic acids, and α-dicarbonyls over the western North Pacific: Sources and formation pathways, Journal of Geophysical Research: Atmospheres, 120, 5010-5035, 10.1002/2014jd022235, 2015.

Carlton, A. G., Turpin, B. J., Lim, H.-J., Altieri, K. E., and Seitzinger, S.: Link between isoprene and secondary organic aerosol (SOA): Pyruvic acid oxidation yields low volatility organic acids in clouds, Geophysical Research Letters, 33, 10.1029/2005gl025374, 2006.

Carlton, A. G., Turpin, B. J., Altieri, K. E., Seitzinger, S., Reff, A., Lim, H.-J., and Ervens, B.: Atmospheric oxalic acid and SOA production from glyoxal: Results of aqueous photooxidation experiments, Atmos. Environ., 41, 7588-7602, 2007.

Carlton, A., Wiedinmyer, C., and Kroll, J.: A review of Secondary Organic Aerosol (SOA) formation from isoprene, Atmos. Chem. Phy., 9, 4987-5005, 2009.

Cheng, C., Wang, G., Meng, J., Wang, Q., Cao, J., Li, J., and Wang, J.: Size-resolved airborne particulate oxalic and related secondary organic aerosol species in the urban atmosphere of Chengdu, China, Atmospheric Research, 161-162, 134-142, 10.1016/j.atmosres.2015.04.010, 2015.

Chow, J. C., Watson, J. G., Chen, L.-W. A., Chang, M. O., Robinson, N. F., Trimble, D., and Kohl, S.: The IMPROVE_A temperature protocol for thermal/optical carbon analysis: maintaining consistency with a long-term database, Journal of the Air & Waste Management Association, 57, 1014-1023, 2007.

Ervens, B.: A modeling study of aqueous production of dicarboxylic acids: 1. Chemical pathways and speciated organic mass production, J. Geophys. Res., 109, 10.1029/2003jd004387, 2004.

Ervens, B., Turpin, B. J., and Weber, R. J.: Secondary organic aerosol formation in cloud droplets and aqueous particles (aqSOA): a review of laboratory, field and model studies, Atmos. Chem. Phys., 11, 11069-11102, 2011.

Fu, T.-M., Jacob, D. J., Wittrock, F., Burrows, J. P., Vrekoussis, M., and Henze, D. K.: Global budgets of atmospheric glyoxal and methylglyoxal, and implications for formation of secondary organic aerosols, J. Geophys. Res., 113, D15303,doi:15310.11029/12007JD009505, 2008.

Gao, S., Ng, N. L., Keywood, M., Varutbangkul, V., Bahreini, R., Nenes, A., He, J., Yoo, K. Y., Beauchamp, J. L., Hodyss, R. P., Flagan, R. C., and Seinfeld, J. H.: Particle phase acidity and oligomer formation in secondary organic aerosol, Environ. Sci. Technol., 38, 6582-6589, 2004.

Gensch, I., Kiendler-Scharr, A., and Rudolph, J.: Isotope ratio studies of atmospheric organic compounds: Principles, methods, applications and potential, International Journal of Mass Spectrometry, 365-366, 206-221, 10.1016/j.ijms.2014.02.004, 2014.

Guo, S., Hu, M., Zamora, M. L., Peng, J., Shang, D., Zheng, J., Du, Z., Wu, Z., Shao, M., Zeng, L., Molina, M. J., and Zhang, R.: Elucidating severe urban haze formation in China, Proceedings of the National Academy of Sciences, 111(49), 17373-17378, 2014.

Hennigan, C. J., Izumi, J., Sullivan, A. P., Weber, R. J., and Nenes, A.: A critical evaluation of proxy methods used to estimate the acidity of atmospheric particles, Atmos. Chem. Phys., 15(5), 2775-2790, 2015.

Ho, K. F., Cao, J. J., Lee, S. C., Kawamura, K., Zhang, R. J., Chow, J. C., and Watson, J. G.: Dicarboxylic acids, ketocarboxylic acids, and dicarbonyls in the urban atmosphere of China, J. Geophys. Res., 112, 10.1029/2006jd008011, 2007.

Ho, K. F., Lee, S. C., Ho, S. S. H., Kawamura, K., Tachibana, E., Cheng, Y., and Zhu, T.: Dicarboxylic acids, ketocarboxylic acids,α-dicarbonyls, fatty acids, and benzoic acid in urban aerosols collected during the 2006 Campaign of Air Quality Research in Beijing (CAREBeijing-2006), J. Geophys. Res., 115, 10.1029/2009jd013304, 2010.

Ho, K. F., Huang, R. J., Kawamura, K., Tachibana, E., Lee, S. C., Ho, S. S. H., Zhu, T., and Tian, L.: Dicarboxylic acids, ketocarboxylic acids, α-dicarbonyls, fatty acids and benzoic acid in $PM_{2.5}$ aerosol collected during CAREBeijing-2007: an effect of traffic restriction on air quality, Atmospheric Chemistry and Physics, 15, 3111-3123, 10.5194/acp-15-3111-2015, 2015.

Hoefs, J., *Stable Isotope Geochemistry.*, Springer, New York, 1997.

Huang, R. J., Zhang, Y., Bozzetti, C., Ho, K. F., Cao, J. J., Han, Y., Daellenbach, K. R., Slowik, J. G., Platt, S. M., Canonaco, F., Zotter, P., Wolf, R., Pieber, S. M., Bruns, E. A., Crippa, M., Ciarelli, G., Piazzalunga, A., Schwikowski, M., Abbaszade, G., Schnelle-Kreis, J., Zimmermann, R., An, Z., Szidat, S., Baltensperger, U., El Haddad, I., and Prevot, A. S.: High secondary aerosol contribution to particulate pollution during haze events in China, Nature, 514, 218-222, 10.1038/nature13774, 2014.

Kawamura, K., and Bikkina, S.: A review of dicarboxylic acids and related compounds in atmospheric aerosols: Molecular distributions, sources and transformation, Atmospheric Research, 170, 140-160, 2016.

Kawamura, K., and Watanabe, T.: Determination of stable carbon isotopic compositions of low molecular weight dicarboxylic acids and ketocarboxylic acids in atmospheric aerosol and snow samples, Analytical Chemistry, 76, 5762-5768, 2004.

Kawamura, K., and Bikkina, S.: A review of dicarboxylic acids and related compounds in atmospheric aerosols: Molecular distributions, sources and transformation, Atmospheric Research, 10.1016/j.atmosres.2015.11.018, 2015.

Kirillova, E. N., Andersson, A., Sheesley, R. J., Kruså, M., Praveen, P. S., Budhavant, K., Safai, P. D., Rao, P. S. P., and Gustafsson, Ö.: ^{13}C- and^{14}C-based study of sources and atmospheric processing of water-soluble organic carbon (WSOC) in South Asian aerosols, J. Geophys. Res., 118, 614-626, 2013.

Li, J., Xie, S. D., Zeng, L. M., Li, L. Y., Li, Y. Q., and Wu, R. R.: Characterization of ambient volatile organic compounds and their sources in Beijing, before, during, and after Asia-Pacific Economic Cooperation China 2014, Atmos. Chem. Phys., 15, 7945-7959, 2015.

Li, W.J. and Shao, L.Y.: Mixing and water-soluble characteristics of particulate organic compounds in individual urban aerosol particles. J. Geophys. Res. 115 (D02301), doi:10.1029/2009JD012575, 2010.

Li, W.J., Zhou, S.Z., Wang, X.F., Xu, Z., Yuan, C., Yu, Y.C., Zhang, Q.Z. and Wang, W.X.: Integrated evaluation of aerosols from regional brown hazes over northern China in winter: Concentrations, sources, transformation, and mixing states. J. Geophys. Res. 116 (D9), doi:10.1029/2010JD015099,2011.

Laskin, A., Laskin, J., and Nizkorodov, S. A.: Chemistry of atmospheric brown carbon, Chem. Rev., 115, 4335-4382, 2015.

Meng, J., Wang, G., Li, J., Cheng, C., Ren, Y., Huang, Y., Cheng, Y., Cao, J., and Zhang, T.: Seasonal characteristics of oxalic acid and related SOA in the free troposphere of Mt. Hua, central China: implications for sources and formation mechanisms, Sci Total Environ, 493, 1088-1097, 2014.

Mu Quan, Z. S.: An evaluation of the economic loss due to the heavy haze during January 2013 in China., China Environmental Science, 33, 2087-2094, 2013.

Pathak, R. K., Wang, T., Ho, K. F., and Lee, S. C.: Characteristics of summertime PM2.5 organic and elemental carbon in four major Chinese cities: Implications of high acidity for water-soluble organic carbon (WSOC), Atmos. Environ., 45, 318-325, 10.1016/j.atmosenv.2010.10.021, 2011.

Rudolph, J., Czuba, E., Norman, A., Huang, L., and Ernst, D.: Stable carbon isotope composition of nonmethane hydrocarbons in emissions from transportation related sources and atmospheric observations in an urban atmosphere, Atmos. Environ., 36, 1173-1181, 2002.

Strader, R., Lurmann, F., and Pandis, S. N.: Evaluation of secondary organic aerosol formation in winter, Atmos. Environ., 33, 4849-4863, 1999.

Sullivan, R. C., and Prather, K. A.: Investigations of the diurnal cycle and mixing state of oxalic acid in individual particles in Asian aerosol outflow, Environ. Sci. Technol., 41, 8062-8069, 2007.

Sun, Y., Wang, Z., Wild, O., Xu, W., Chen, C., Fu, P., Du, W., Zhou, L., Zhang, Q., Han, T., Wang, Q., Pan, X., Zheng, H., Li, J., Guo, X., Liu, J., and Worsnop, D. R.: "APEC Blue": Secondary Aerosol Reductions from Emission Controls in Beijing, Scientific reports, 6, 20668, 10.1038/srep20668, 2016.

Surratt, J. D., Lewandowski, M., Offenberg, J. H., Jaoui, M., Kleindienst, T. E., Edney, E. O., and Seinfeld, J. H.: Effect of Acidity on Secondary Organic Aerosol Formation from Isoprene, Environ. Sci. Technol., 41, 5363-5369, 2007.

Surratt, J. D., Chan, A. W. H., Eddingsaas, N. C., Chan, M., Loza, C. L., Kwan, A. J., Hersey, S. P., Flagan, R. C., Wennberg, P. O., and Seinfeld, J. H.: Reactive intermediates revealed in secondary organic aerosol formation from isoprene, Proceedings of National Academy of Science of United States of America, 107, 6640-6645, 2010.

Tang, G., Zhu, X., Hu, B., Xin, J., Wang, L., Münkel, C., Mao, G., and Wang, Y.: Impact of emission controls on air quality in Beijing during APEC 2014: lidar ceilometer observations, Atmos. Chem. Phys., 15, 12667-12680, 2015.

Tilgner, A. and Herrmann, H.: Radical-driven carbonyl-to-acid conversion and acid degradation in tropospheric aqueous systems studied by CAPRAM. Atmos. Environ., 44, 5415-5422, 2010.

Van Donkelaar, A., Martin, R. V., Brauer, M., Kahn, R., Levy, R., Verduzco, C., and Villeneuve, P. J.: Global estimates of ambient fine particulate matter concentrations from satellite-based aerosol optical depth: development and application, University of British Columbia, 2015.

van Pinxteren, D., Neusüß, C., and Herrmann, H.: On the abundance and source contributions of dicarboxylic acids in size-resolved aerosol particles at continental sites in central Europe, Atmos. Chem. Phys., 14, 3913-3928, 2014.

Wang, G., Cheng, C., Meng, J., Huang, Y., Li, J. and Ren, Y.: Field observation on secondary organic aerosols during Asian dust storm periods: Formation mechanism of oxalic acid and related compounds on dust surface. Atmos. Environ., 113, 169-176, 2015.

Wang, G. H., Kawamura, K., Lee, S. C., Ho, K. F. and Cao, J. J.: Molecular, seasonal and spatial distributions of organic aerosols from fourteen Chinese cities. Environ. Sci. Technol., 40, 4619-4625, 2006.

Wang, G., Kawamura, K., Umemoto , N., Xie, M., Hu, S. and Wang, Z.: Water-soluble organic compounds in PM2.5 and size-segregated aerosols over Mt. Tai in North China Plain. Journal of Geophysical Research-Atmospheres, 114, D19208, dio.10.1029/2008JD011390, 2009.

Wang, G., Kawamura, K., Cheng, C., Li, J., Cao, J., Zhang, R., Zhang, T., Liu, S., and Zhao, Z.: Molecular distribution and stable carbon isotopic composition of dicarboxylic acids, ketocarboxylic acids, and alpha-dicarbonyls in size-resolved atmospheric particles from Xi'an City, China, Environ. Sci. Technol., 46, 4783-4791, 2012.

Wang, G., Niu, S, Liu, C., and Wang, L.: Identification of dicarboxylic acids and aldehydes of PM10 and PM2.5 aerosols in Nanjing, China, Atmospheric Environment, 36(12), 1941-1950, 2002.

Wang, G., Xie, M., Hu, S., Gao, S., Tachibana, E., and Kawamura, K.: Dicarboxylic acids, metals and isotopic compositions of C and N in atmospheric aerosols from inland China: implications for dust and coal burning emission and secondary aerosol formation, Atmos. Chem. Phys., 10, 6087-6096, 2010.

Wang, G., Wang, J., Ren, Y. and Li, J.: Chemical characterization of organic aerosols from Beijing during the 2014 APEC (under preparation), 2016.

Wang, G., Zhang, R., Zamora, M. L., Gomez, M. E., Yang, L., Hu, M., Lin, Y., Guo, S., Meng, J., Li, J., Cheng, C., Hu, T., Ren, Y., Wang, Y., Gao, J., Cao, J., An, Z., Zhou, W., Jiayuan Wang, Marrero-Ortiz, W., Tian, P., Secrest, J., Peng, J., Du, Z., Jing Zheng, Shang, D., Zeng, L., Shao, M., Wang, W., Huang, Y., Wang, Y., Zhu, Y., Li, Y., Hu, J., Pan, B., Cai, L., Cheng, Y., Rosenfeld, D., Liss, P. S., Duce, R. A., Kolb, C. E., and Molina, M. J.: Persistent Sulfate Formation from London Fog to Chinese Haze, Proceedings of National Academy of Science of United States of America, doi/10.1073/pnas.1616540113., 2016.

Wang, Y., Zhang, Q. Q., He, K., Zhang, Q., and Chai, L.: Sulfate-nitrate-ammonium aerosols over China: response to 2000–2015 emission changes of sulfur dioxide, nitrogen oxides, and ammonia, Atmos. Chem. Phys., 13, 2635-2652, 2013.

Weber, R. J., Guo, H., Russell, A. G., and Nenes, A.: High aerosol acidity despite declining atmospheric sulfate concentrations over the past 15 years, Nature Geoscience, 9, 282-285, 10.1038/ngeo2665, 2016.

Wei, X., Gu, X., Chen, H., Cheng, T., Wang, Y., Guo, H., Bao, F., and Xiang, K.: Multi-Scale Observations of Atmosphere Environment and Aerosol Properties over North China during APEC Meeting Periods, Atmosphere, 7(1), 2016.

Xing, L., Fu, T. M., Cao, J. J., Lee, S. C., Wang, G. H., Ho, K. F., Cheng, M. C., You, C. F., and Wang, T. J.: Seasonal and spatial variability of the OM/OC mass ratios and high regional correlation between oxalic acid and zinc in Chinese urban organic aerosols, Atmos. Chem. Phys., 13, 4307-4318, 2013.

512 Xu, W. Q., Sun, Y. L., Chen, C., Du, W., Han, T. T., Q.Wang, Q., Fu, P. Q., F.Wang, Z., Zhao, X. J., Zhou, L. B., Ji,
513 D. S., Wang, P. C., and Worsnop, D. R.: Aerosol composition, oxidation properties, and sources in Beijing:
514 results from the 2014 Asia-Pacific Economic Cooperation summit study, Atmos. Chem. Phys., 15, 13681–13698,
515 2015.
516 Yu, J. Z., Huang, X.-F., Xu, J., and Hu, M.: When Aerosol Sulfate Goes Up, So Does Oxalate: Implication for the
517 Formation Mechanisms of Oxalate, Environ. Sci. Technol., 39, 128-133, 2005.
518 Zhang, Q., Jimenez, J. L., Worsnop, D. R., and Canagaratna, M.: A case study of urban particle acidity and its
519 influence on secondary organic aerosol, Environ. Sci. Technol., 41, 3213-3219, 2007.
520 Zhang, Q., Streets, D. G., Carmichael, G. R., He, K., Huo, H., Kannari, A., Klimont, Z., Park, I., Reddy, S., and Fu,
521 J.: Asian emissions in 2006 for the NASA INTEX-B mission, Atmos. Chem. Phys., 9, 5131-5153, 2009.
522 Zhang, R., Wang, G., Guo, S., Zamora, M. L., Ying, Q., Lin, Y., Wang, W., Hu, M., and Wang, Y.: Formation of
523 urban fine particulate matter, Chemical Reviews, 115, 3803-3855, 2015.
524 Zheng, G. J., Duan, F. K., Su, H., Ma, Y. L., Cheng, Y., Zheng, B., Zhang, Q., Huang, T., Kimoto, T., Chang, D.,
525 Pöschl, U., Cheng, Y. F., and He, K. B.: Exploring the severe winter haze in Beijing: the impact of synoptic
526 weather, regional transport and heterogeneous reactions, Atmos. Chem. Phys., 15, 2969-2983, 2015.
527

Figure Captions

Figure 1. Temporal variations of meteorological conditions, gaseous pollutants and major components of $PM_{2.5}$ during the 2014 APEC campaign. (The brown shadows represent two air pollution events characterized by highest $PM_{2.5}$ levels before- and after-APEC, while the blue shadow represents the APEC event).

Figure 2. Chemical composition of $PM_{2.5}$ during the 2014 APEC campaign.

Figure 3. Molecular distributions of dicarboxylic acids and related compounds in $PM_{2.5}$ of Beijing, China during the 2014 APEC campaign. The pie chart is the average composition of total detected organic compounds (TDOC) and the top number is the average mass concentration of TDOC of the whole study period.

Figure 4. Compositions of total detected organic compounds (TDOC) in $PM_{2.5}$ during the 2014 APEC campaign.

Figure 5. Correlation analysis for oxalic acid (C_2) and sulfate in $PM_{2.5}$ during the whole 2014 APEC campaign. (**a-c**) Concentrations of C_2 with sulfate, relative humidity (RH), and aerosol liquid water content (ALWC); (**d, e**) sulfate and C_2 with aerosol acidity [H^+] and (**f**) temperature with mass ratio of C_2 to total detected organic compounds (C_2/TDOC).

Figure 6. (**a**) 72-h backward trajectories determined by the National Oceanic and Atmospheric Administration Hybrid Single Particle Lagrangian Integrated Trajectory (HYSPLIT) model arriving at the sampling site to reveal the major air mass flow types during the study period. Northwesterly wind (light blue) was most frequently (64%), followed by northerly (21%, pink) and southerly (15%, black) and is defined as clean, mixed and polluted types, respectively (see the definitions in the text); (**b**) Time series of $\delta^{13}C$ values and concentration of oxalic acid during the whole study period (Colors in Fig. 6a are corresponding to those in Fig. 6b).

Figure 7. Comparison of chemical composition of $PM_{2.5}$ during two air pollution events.(**a**) Percentages of major species in $PM_{2.5}$; (**b,** c) mass ratios of major species and organic tracers in $PM_{2.5}$; (**d**) stable carbon isotope composition of oxalic acid (C_2) (Data about levoglucosan (Lev), PAHs and hopanes are cited from Wang et al (2016)).

Table 1. Meteorological parameters and concentrations of gaseous pollutants and chemical components of $PM_{2.5}$ in Beijing during the 2014 APEC campaign

	Whole period (N=48)	Before-APEC (08/10−02/11) (N=26)	During-APE (03/11−12/11) (N=10)	After-APEC (13/11−14/11) (N=12)
I. Meteorological parameters				
Temperature, °C	9.5± 4.3 (3.0−18)	13±2.6 (9.0−18)	7.0±1.7 (4.0−10)	4.3±1.3 (3.0−7.0)
Relative humidity,	56±19 (17−88)	62±19 (22−88)	47±14 (17−65)	51±16 (29−80)
Visibility, km	8.8±6.8 (1.0−28)	7.3±6.6 (1.0−24)	13±7.7 (6.0−28)	7.2±4.2 (2.0−15)
Wind speed, km h^{-1}	8.0±4.9 (3.0−26)	7.6±4.8 (3.0−26)	9.4±6.6 (3.0−26)	7.8±2.9 (3.0−13)
II. Gaseous pollutants, μg m^{-3}				
O_3	48 ± 23 (6.0−115)	55 ± 24 (9.0−115)	52 ± 13 (25−69)	29 ± 18 (6.0−60)
SO_2	12 ± 8.5 (2.0−43)	8.8 ± 4.6 (2.0−19)	7.6 ± 3.9 (2.0−15)	23 ± 8.8 (13−43)
NO_2	68±29 (10−135)	71 ± 27 (22−118)	45 ± 18 (10−69)	78 ± 29 (45−135)
CO	1360±730 (220−3320)	1370 ± 700 (250−2460)	960 ± 410 (220−1420)	1720 ± 830 (740−3320)
III. Major components of $PM_{2.5}$, μg m^{-3}				
$PM_{2.5}$	157 ± 110 (16−408)	178 ± 122 (16−408)	98 ± 46 (28−183)	161 ± 100 (36−383)
SO_4^{2-}	12 ± 11.5 (1.2−43)	15 ± 13 (1.2−43)	5.3 ± 2.8 (1.8−11)	11 ±10 (2.9−34)
NO_3^-	21 ± 22 (0.32−88)	28 ± 26 (0.32−88)	10 ±8.1 (1.2−26)	15 ± 13 (2.9−46)
NH_4^+	7.3± 7.2 (0.2−28)	9.0 ± 8.0 (0.2−28)	3.1 ± 2.6 (0.2−8.6)	6.9 ± 6.4 (1.0−22)
OC	28 ± 18 (5.7−78)	26 ± 16 (6.0−67)	19 ± 7.6 (5.7−29)	39 ± 23 (9.7−78)
EC	8.8 ± 5.4 (1.4−25)	8.6 ± 4.6 (1.4−18)	6.0 ± 2.7 (1.5−9.6)	12 ± 7.0 (2.1−25)
WSOC	10 ± 6.0 (2.4−32)	11± 4.6 (3.1−32)	6.4 ± 2.6 (2.4−11)	11 ± 6.1 (4.5−24)
ALWC	40 ± 62 (0−299)	58 ± 75 (0−299)	6.3± 5.5 (0−19)	28 ± 41 (0.4−136)
$[H^+]$	0.083 ± 0.14(0−0.56)	0.13 ± 0.17 (0−0.56)	0.026 ± 0.025 (0−0.072)	0.033 ± 0.067 (0−0.20)

592
593

Table 2. Concentrations of dicarboxylic acids and related compounds in $PM_{2.5}$ in Beijing during the 2014 APEC campaign (ng m^{-3})

	Whole period (N=48)	Before-APEC (08/10−02/11) (N=26)	During-APE (03/11−12/11) (N=10)	After-APEC (13/11−14/11) (N=12)
		I. Dicarboxylic acids		
Oxalic, C_2	334 ± 461 (10−2127)	502 ± 564 (10.5−2127)	101 ± 69 (35−251)	166 ± 157 (22−554)
Malonic, C_3	31 ± 42 (ND−247)	45.7 ± 52.1 (1.44−247)	12 ± 8.0 (3.4−22.8)	16± 10.9 (ND−36)
Succinic, C_4	74 ± 118 (3.0−722)	111 ± 150 (3.0−722)	24 ± 14 (7.1−42)	36 ± 26 (4.9−90)
Glutaric, C_5	8.7 ± 12 (ND−68)	13± 15 (ND−68.1)	2.9 ± 2.24 (0.9−5.8)	4.9 ± 4.2 (ND−13)
Adipic, C_6	13± 14 (0.9−83)	17 ± 18 (1.9−83)	5.9 ±3.8 (2.1−14)	9.9 ± 7.1 (2.0−23)
Pimelic, C_7	2.1 ± 3.8 (ND−27)	2.6 ± 5.1(ND−27)	1.1 ± 0.7(0.2−2.3)	2.0 ± 1.1 (0.9−4.4)
Suberic, C_8	10 ± 11 (ND−66)	12± 13 (ND−66)	7.6 ± 5.0 (1.3−16)	8.7 ± 6.0(2.0−21)
Azelaic, C_9	5.0± 4.9(0.5−21)	6.4 ± 5.7 (0.6−21)	1.7± 0.9 (0.5−3.2)	4.6 ± 3.3 (1.3−13)
Sebacic, C_{10}	7.7 ± 7.4 (ND−34)	9.4 ± 8.8 (ND−34)	4.2± 3.6 (0.5−11)	6.8 ± 4.9 (1.4−16)
Undecanedioic, C_{11}	11 ± 13 (ND−77)	14 ± 16 (ND−77)	3.3 ± 2.5 (ND−7.5)	9.4 ± 6.4 (0.8−23)
Methylsuccinic, iC_5	13 ± 16 (0.6−79)	18 ± 19 (0.6−79)	4.8 ± 3.0 (1.0−9.2)	8.4 ± 6.0(2.3−19)
Methyglutaric, iC_6	7.5 ± 10 (ND−36)	11± 12 (ND−36)	0.9 ± 09 (ND−2.6)	4.6± 5.1 (ND−14)
Maleic, M	3.4 ± 3.9 (ND−15)	4.6± 4.7 (ND−15)	1.4 ± 0.8 (ND−2.9)	2.4 ± 2.0 (ND−6.3)
Fumaric, F	7.2 ± 8.8 (ND−64)	10 ± 11 (ND−64)	2.2 ± 1.5 (ND−5.4)	4.7 ± 3.2 (1.4−10)
Phthalic, Ph	17 ± 14 (1.5−64)	20 ± 16 (1.5−64)	10 ± 6.8 (2.3−20)	17 ± 9.0 (6.4−31)
Isophthalic, iPh	2.1 ± 2.5 (ND−10)	2.9 ± 2.8 (ND−10)	2.0 ± 2.1 (0.2−5.9)	0.5 ± 0.3 (ND−3.2)
Terephthalic, tPh	46 ± 35 (2.6−133)	50 ± 35 (2.6−123)	28 ± 19(4.7−59)	53± 40 (7.4−133)
Subtotal	593 ± 739 (25−3788)	849 ± 905 (25−3788)	214 ± 135 (72−447)	354 ± 279 (85−965)
		II. Keto-carboxylic acids		
Pyruvic, Pyr	24 ± 20 (1.3−84)	31± 23 (2.4−84)	15 ± 12 (1.3−36)	15 ± 9.3 (3.2−33)
Glyoxylic, ωC_2	33 ± 51 (1.2−300)	48± 64 (1.2−300)	10 ± 7.7 (2.6−21)	20 ± 23 (2.8−80)
7-Oxoheptanoic, ωC_7	8.8 ± 14 (ND−90)	13 ± 17 (ND−90)	4.2 ± 3.6 (ND−13)	4.5 ± 5.1 (ND−17)
Subtotal	66 ± 81 (3.6−474)	92 ± 99 (3.6−474)	30 ± 22 (5.9−66)	40 ± 35 (13−128)
		III α-Dicarbonyls		
Glyoxal, Gly	44 ± 47 (4.2−270)	57 ± 56 (4.2−270)	22 ± 19 (4.9−47)	35 ± 30 (7.3−101)
Methylglyoxal, mGly	82 ± 82 (ND−406)	102 ± 96 (ND−406)	60 ± 52 (15−139)	58 ± 51 (5.8−144)
Subtotal	126 ± 115 (5.3−466)	158 ± 132 (5.3−466)	81.6 ± 67.4 (22−186)	93 ± 80 (14−225)
TDOC[b]	785 ± 872 (36−4636)	1099 ± 1104 (36−4636)	325 ± 220 (107−664)	487 ± 387 (117-1318)

[a]ND: not detectable; [b]TDOC: total detected organic compounds.

Table 3 Linear correlation coefficients of $\delta^{13}C$ of C_2 with $C_2/\omega C_2$, C_2/mGly, and TDOC/WSOC

	$C_2/\omega C_2$	C_2/mGly	TDOC/WSOC
$\delta^{13}C$	0.49**	0.35*	0.41*

** $p<0.01$; * $p<0.05$

598

Table 4. Meteorological parameters and chemical compositions (μg m^{-3}) of two maximum $PM_{2.5}$ between two pollution episodes in Beijing

	T (°C)	RH (%)	V[a] (km)	$PM_{2.5}$	OC	EC	SIA[b]	TDOC[c]
Event I (8/10-11/10, Before-APEC)	16.7 ± 0.8	82 ± 4	1.5 ± 0.5	349 ± 57	45 ± 12	12 ± 2	106±39	2749 ± 1357
Event II (18/11-21/11, After-APEC)	4.5 ± 1.7	62 ± 13	3.5 ± 1.5	259 ± 102	60 ± 21	17 ± 6	60±32	831 ± 400

[a]V: visibility; [b]SIA: secondary inorganic ions (the sum of sulfate, nitrate and ammonium); [c]TDOC: total detected organic compounds

599

600

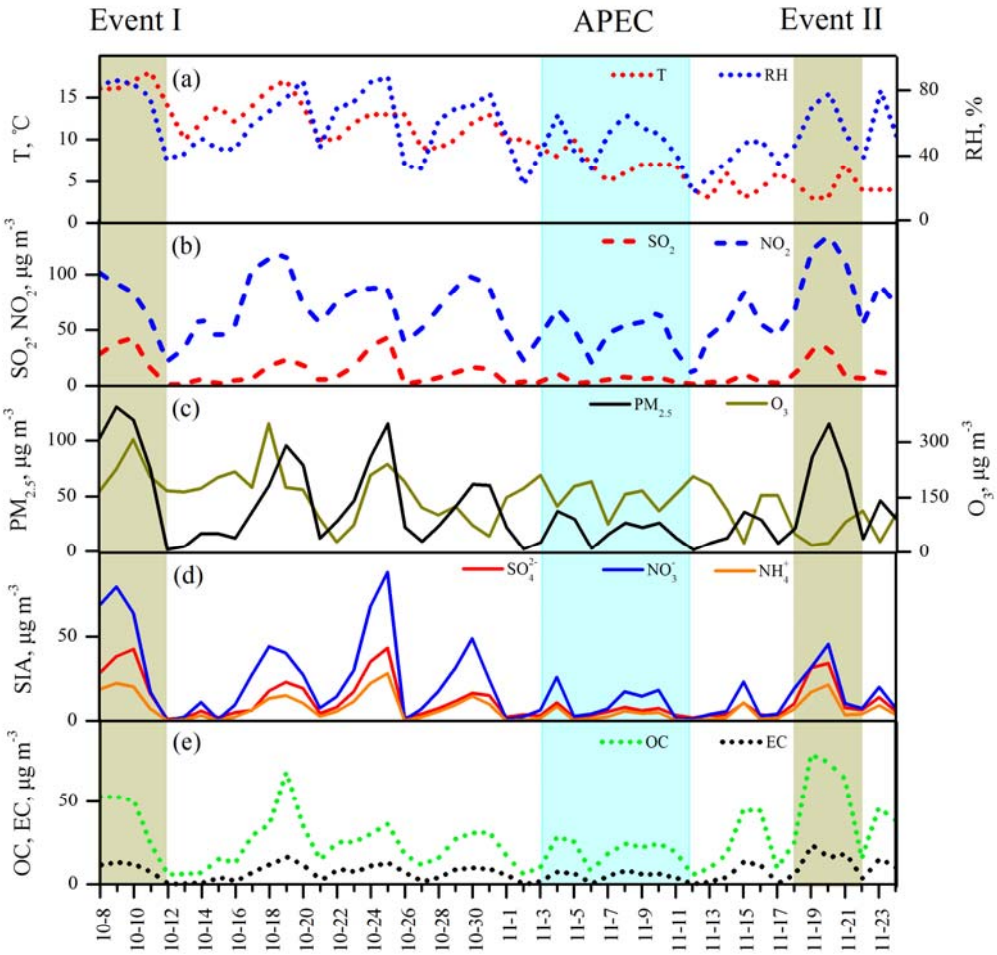

601

602 **Figure** 1. Temporal variations of meteorological conditions, gaseous pollutants and major components of $PM_{2.5}$
603 during the 2014 APEC campaign. (The brown shadows represent two air pollution events characterized
604 by highest $PM_{2.5}$ levels before- and after-APEC, while the blue shadow represents the APEC event).

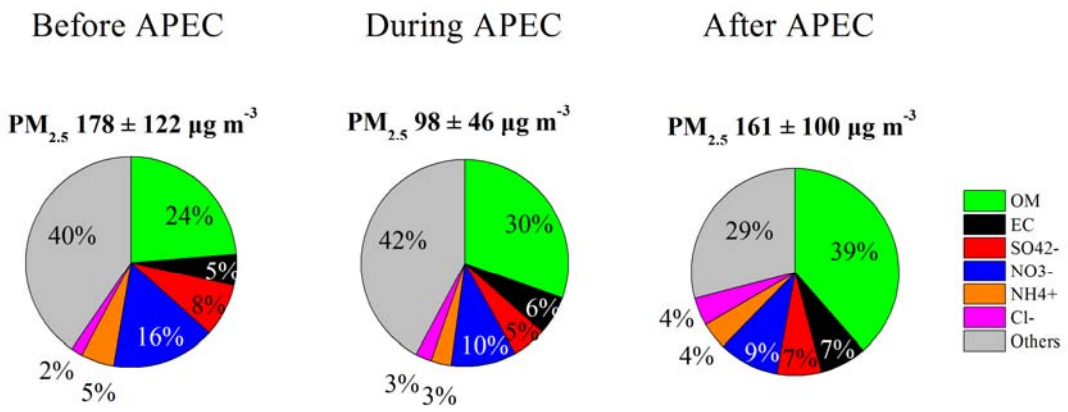

605

606 **Figure 2.** Chemical composition of $PM_{2.5}$ during the 2014 APEC campaign.

607

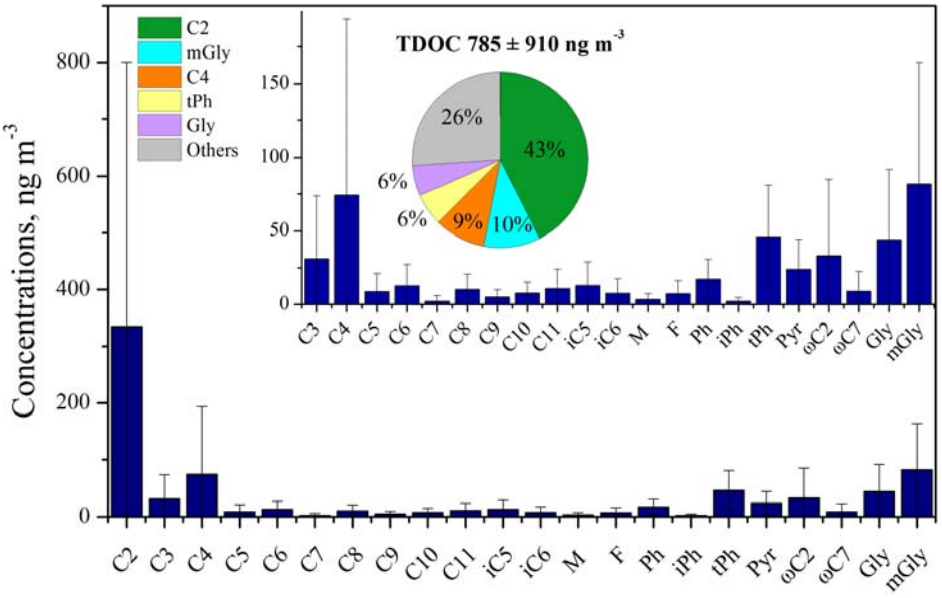

Figure 3. Molecular distributions of dicarboxylic acids and related compounds in $PM_{2.5}$ of Beijing, China during the 2014 APEC campaign. The pie chart is the average composition of total detected organic compounds (TDOC) and the top number is the average mass concentration of TDOC of the whole study period.

614

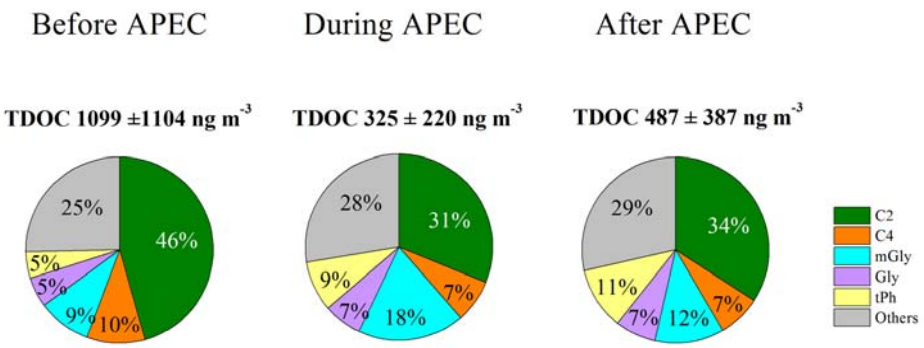

615

616 **Figure 4**. Compositions of total detected organic compounds (TDOC) in $PM_{2.5}$ during the 2014 APEC campaign.

617

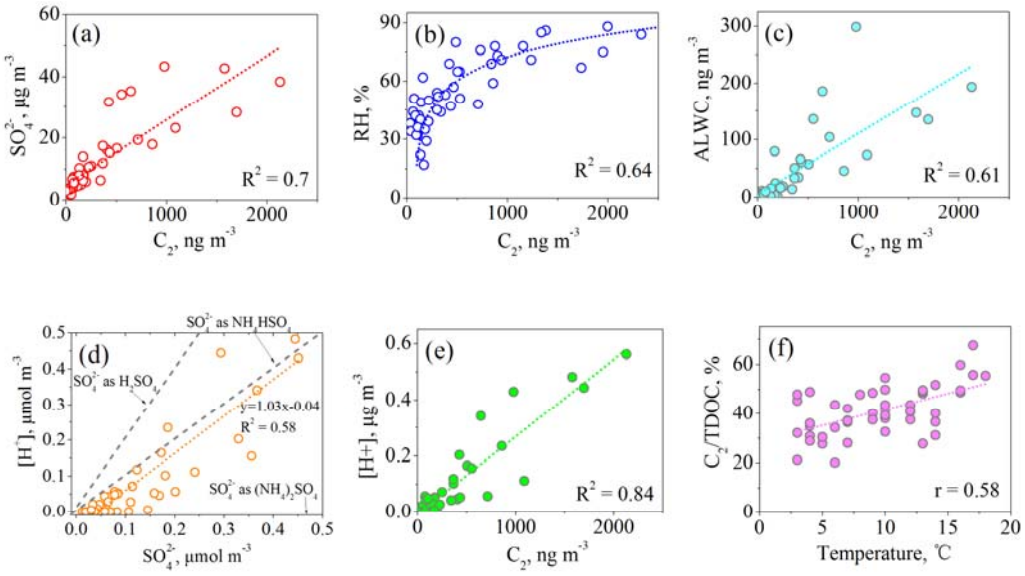

Figure 5. Correlation analysis for oxalic acid (C_2) and sulfate in $PM_{2.5}$ during the whole 2014 APEC campaign. (**a-c**) Concentrations of C_2 with sulfate, relative humidity (RH), and aerosol liquid water content (ALWC); (**d, e**) sulfate and C_2 with aerosol acidity [H^+] and (**f**) temperature with mass ratio of C_2 to total detected organic compounds (C_2/TDOC).

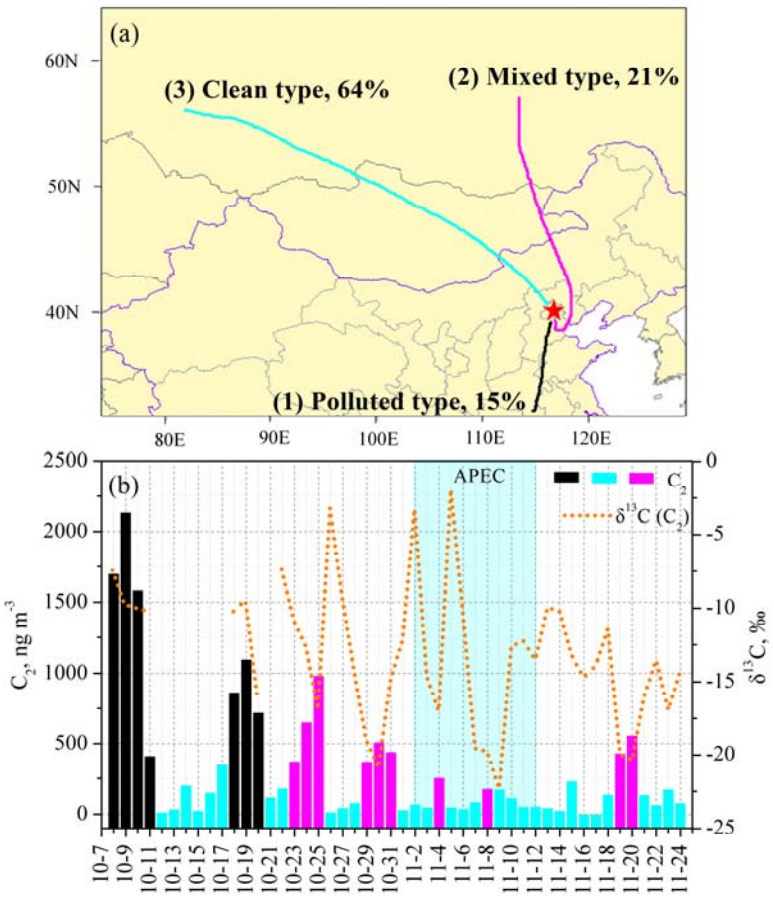

Figure 6. (**a**) 72-h backward trajectories determined by the National Oceanic and Atmospheric Administration Hybrid Single Particle Lagrangian Integrated Trajectory (HYSPLIT) model arriving at the sampling site to reveal the major air mass flow types during the study period. Northwesterly wind (light blue) was most frequently (64%), followed by northerly (21%, pink) and southerly (15%, black) and is defined as clean, mixed and polluted types, respectively (see the definitions in the text); (**b**) Time series of $\delta^{13}C$ values and concentration of oxalic acid during the whole study period (Colors in Fig. 6a are corresponding to those in Fig. 6b).

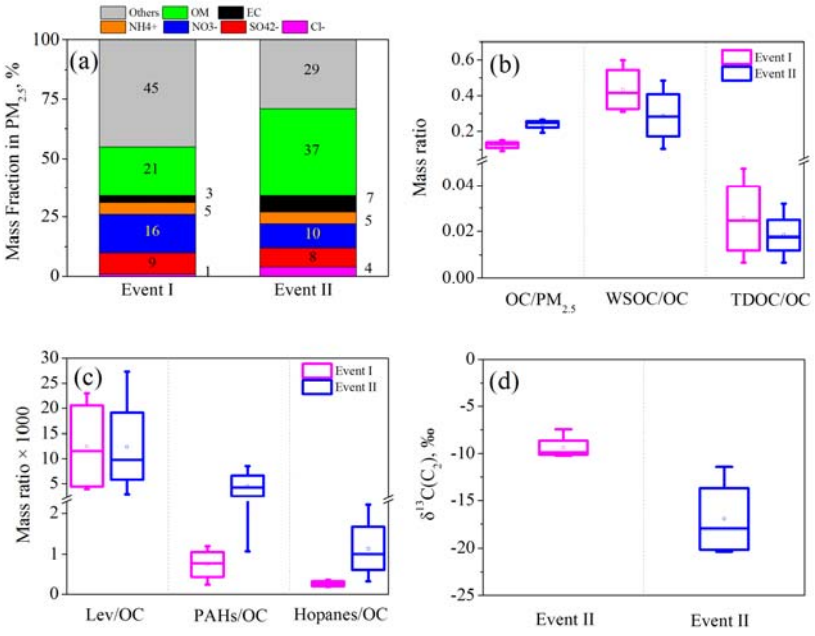

Figure 7. Comparison of chemical composition of $PM_{2.5}$ during two air pollution events.(**a**) Percentages of major species in $PM_{2.5}$; (**b**, **c**) mass ratios of major species and organic tracers in $PM_{2.5}$; (**d**) stable carbon isotope composition of oxalic acid (C_2) (Data about levoglucosan (Lev), PAHs and hopanes are cited from Wang et al (2016)).